TRANSACTIONS OF THE INSTITUTE OF FLUID-FLOW MACHINERY

No. 128, 2015, 97–118

KINGA STRĄK[1] and MAGDALENA PIASECKA

A study of flow boiling heat transfer in a rectangular minichannel using liquid crystal and infrared thermography

Kielce University of Technology, Aleja Tysiąclecia Państwa Polskiego 7, 25-314 Kielce, Poland

Abstract

This paper presents results of flow boiling heat transfer in two parallel asymmetrically heated vertical minichannels. The heating element for Fluorinert FC-72 flowing in the minichannels was a thin foil with an enhanced surface on the side in contact with the fluid. The channels were observed from both sides through glass panes. Two of the panes allowed us to observe the two phase flow patterns on the enhanced surface of the foil, while the other two panes were used for simultaneous measurement of temperature on the smooth side of the foil. The temperature was measured by applying two contactless methods. One was liquid crystal thermography (LCT), which required treating the foil surface with thermochromic liquid crystals (TLCs), and the other was infrared thermography (IRT), which required coating the foil surface with black paint. Calculations were performed on the basis ofa one-dimensional model to determine the heat transfer coefficient at the foil-fluid interface from the Robin boundary condition. The experimental results were graphically represented as the foil temperature and the heat transfer coefficient against the distance from the minichannel inlet and as LCT and IRT images obtained for saturated boiling.

Keywords: Flow boiling heat transfer; Rectangular minichannel; Enhanced foil surface; Liquid crystal thermography; Infrared thermography

Nomenclature

A – surface area, m^2

[1]E-mail address: kzietala@tu.kielce.pl

C_0 – confinement number
d – diameter, m
d_h – hydraulic diameter, m
g – gravitational acceleration, m/s^2
I – current, A
L – length of the minichannel, m
n – derivative of temperature in the direction normal to the isothermal surface, m
p – pressure, N/m^2
q_w – density of the heat flux, W/m^2
q_{wl} – density of the heat flux for heat transferred from the heating foil to the surroundings, W/m^2
T – temperature, K
x – distance from the minichannel inlet, m

Greek symbols

α – heat transfer coefficient, $W/(m^2K)$
δ – thickness, m
ΔU – voltage drop, V
λ – thermal conductivity, W/(mK)
ρ_l – density of the saturated liquid, kg/m^3
ρ_ν – density of the saturated vapour, kg/m^3
σ – surface tension, N/m

Subscripts

cond – conduction
conv – convection
in – inlet
F – foil
f – fluid
G – glass
h – hydraulic
out – outlet
sat – saturation
w – wall

Superscripts

LCT – liquid crystal thermography
IRT – infrared thermography

1 Introduction

Today heat exchangers are miniaturized to reduce their size and cost; however, their efficiency needs to be as high as possible. Flow boiling heat transfer is a process during which the important parameters, i.e., the heat

transfer coefficient and the heat flux, reach very high values. Because of the change in the state of matter, which is accompanied by flow boiling heat transfer, the highest heat flux occurs when the difference in temperature between the heating surface and the saturated liquid is small. The use of enhanced surfaces is reported to improve the efficiency of the heat transfer process [1]. Recently there has been an increased interest in flow boiling heat transfer in minichannels. Research on flow boiling heat transfer in minichannel has gained significant attention in engineering community because of the utilization of latent heat of vapourization in their compact sizes Miniaturization has become a prerequisite in the design of energy and process systems, including compact heat exchangers, cooling devices, high-powered lasers, and microelectronic manufacturing systems. Compact heat exchangers with small channels are able to provide good surface contact even under high pressure conditions. When microscale channels are used for flow boiling, larger amounts of thermal energy can be removed than during single-phase flow. Capillary forces and surface tension play an important role in two-phase flow and heat transfer. There are visible differences in flow between macrochannels and minichannels [2].

There are many criteria taken into account when classifying small channels. Kandlikar and Grande, for example, divide channels according to their hydraulic diameter, (d_h), into three groups [3]:

a) conventional channels: $d_h > 3$ mm,

b) minichannels: 200 μm $\leq d_h \leq 3$ mm,

c) microchannels: 10μm $\leq d_h \leq 200$ μm.

Another classification based on the hydraulic diameter was proposed by Shah. It is used for channels incompact heat exchangers, and these fall into two groups [4]:

a) conventional channels: $d_h > 6$ mm,

b) minichannels: $d_h < 6$ mm.

On the other hand, Kewand Cornwell suggests that the division into micro- and macrochannels should be based on the confinement number, which is defined by [5]

$$\mathrm{C}_0 = \frac{1}{d_h}\sqrt{\frac{\sigma}{g(\rho_l - \rho_\nu)}}\,. \tag{1}$$

With the confinement number as the criterion, channels are categorized into:

a) microchannels, for $C_0 < 0.5$,

b) macrochannels, for $C_0 > 0.5$.

In Poland, the problems of flow boiling heat transfer have been studied by several research teams. One of the teams, headed by Bohdal of the Koszalin University of Technology, deals with the behavior of refrigerants, especially their phase changes. Their main area of interest is heat transfer in conventional channels [6–8], but recently they have also analyzed minichannels [9–11]. Dutkowski of the Koszalin University of Technology is another researcher involved in the study of heat transfer [12–15], who specializes in the heat transfer and flow resistance during two-phase flow of water and refrigerants in a minichannel with a circular cross-section. His findings concern heat transfer phenomena ina 500 mm long minichannel with a diameter ranging from 0.21 mm to 2.3 mm for different fluids: air, water, water-air mixture, and cooling liquids (R-134a and R-404A).

The next research team, headed by Mikielewicz of the Gdańsk University of Technology, is involved in experimental and theoretical investigations of flow boiling heat transfer in minichannels [16–19]. Their studies focus on flow boiling heat transfer for R-123 in a circular cross-section channel with a diameter of 1.15 mm and 2.3 mm and a length of 380 mm, whose surface is enhanced or smooth. They also propose a semi-empirical model to determine the heat transfer coefficient.

The studies undertaken by Cieśliński's team of the Gdańsk University of Technology concern pool and flow boiling on enhanced surfaces [20–24]. They conducted experiments for pure R22, R134a, R407C and their mixtures with synthetic oil (FuchS Reniso Triton SEZ 32) flowing in a stainless steel tube with a porous or smooth inside surface. In the case of flow boiling heat transfer with pure refrigerants, the heat transfer coefficient was higher and the pressure drop was lower for a porous coated surface than for a smooth surface at the same mass velocity. They proposed a correlation equation for calculating the heat transfer coefficient during the flow boiling heat transfer of pure refrigerants in a tube with a porous coated inside surface.

The flow boiling heat transfer in a short minichannel with a circular cross-section was studied by Wilk [23] of the Rzeszów University of Technology. Her experiments concerned convective mass and heat transfer at low Reynolds numbers [26].

Ciałkowski and Frąckowiak of the Poznań University of Technology deal with direct and inverse problems in mechanics and inverse problems in heat

conduction. In [27], they apply the Trefftz method to solve the problem of unsteady motion of a viscous liquid.

The research team of the Kielce University of Technology, headed by Poniewski, (for years 1991–2008) includes Orzechowski, Wójcik, Pastuszko, Piasecka, and Poniewski is now head of a research team at the Płock Satellite Institute of the Warsaw University of Technology. The research of the Kielce team focuses on pool boiling and flow boiling heat transfer in minichannels with enhanced and smooth surfaces of the heating foil. Orzechowski, Wójcik and Pastuszko deal with the problems of pool boiling heat transfer. Orzechowski and Tyburczyk [28–30] are concerned with pool boiling heat transfer on fins with mesh structures. Wójcik [31–33] investigates the incipience of boiling and heat transfer hysteresis on porous coatings; now he is working with a research team at the AGH University of Science and Technology. Pastuszko [34–37] studies pool boiling heat transfer on fin- and microfin and tunnel structures. The main are as of interest of Piasecka [38–47] are boiling heat transfer and two-phase flow pressure drop in minichannels with smooth and enhanced surfaces at different orientations. Piasecka, Maciejewska and Hożejowska have proposed several models for determining the heat transfer coefficient and the application of the Trefftz method to determine the temperature fields and the heat transfer coefficient in flow boiling in minichannels [46,47,55]. Finally, Kaniowski [48,49] analyzes two-phase flow patterns in a vertical minichannel with a smooth inside surface.

This study involved calculating the heat transfer coefficient at the foil-fluid interface with the one dimensional model using the data obtained experimentally from two contactless temperature measurement methods, i.e., liquid crystal thermography and infrared thermography. The results are presented as liquid crystal thermography (LCT) and infrared thermography (IRT) images, as well as the curves of the local temperature of the heating surface vs. distance from the inlet and curves of the local heat transfer coefficient vs. distance from the inlet obtained for saturated boiling.

2 Experimental setup

The experimental setup consists of several systems: the test loop fluid FC-72, the calibration loop, the lighting system, the data and image acquisition system and the supply and control system, as shown in Fig. 1.

The test loop in which Fluorinert FC-72 circulates are composed of a heat exchanger, a rotary pump, rotameters, a compensating tank, a filter,

and a deaerator. The calibration loop, where water circulates, comprises a rotary pump, a filter, a deaerator, a heater with an electric heating element and a digital camera. In the lighting system there are two types of lamps: halogen lamps to light two phase flow patterns and fluorescent cold light tubes to illuminate the other side of the parallel minichannels. The data and image acquisition system designed to collect measurement data is made up of a data acquisition station with a computer and appropriate software, an infrared camera, a digital camera, and a digital single-lens reflex (SLR) camera. Another important system of the experimental setup is the supply and control system, which consists of an inverter welder, a shunt, an ammeter and a voltmeter.

The most important element of the setup is the test section with two parallel vertically-oriented rectangular minichannels, each 1.8 mm deep, 24 mm wide, and 360 mm long. The schematic diagrams of the test section are shown in Fig. 2. The heating element for FC-72 flowing in each minichannel (1) is a Haynes-230 alloy foil with a thickness of about 0.1 mm (2). The surface of the foil in contact with the fluid is enhanced. The channel can be observed through four glass panes. The first pane (4a) enables us to monitor changes in temperature on the smooth surface of the foil because it is coated with thermochromicliquid crystals (TLCs) (3). In this paper, this minichannel (Fig. 2a) will be called the LCT minichannel. In the other minichannel, changes in temperature are observed using infrared thermography. For this purpose, the foil was coated with blackpaint (9) to achieve an emissivity of 0.83 [50]. Temperature is measured with an infrared camera in the central,axially symmetric part of the channel (approx. 10 mm $\times$ 350 mm). The sides of the channel are reinforced with glass panels to prevent the heating foil from deformation. The other minichannel (Fig. 2b) will be called the infrared (IRT) minichannel. The other side of the minichannels, where two-phase flow patterns occur on the enhanced surface of the foil in contact with the fluid (8), can be observed through the other two glass panes. Pressure converters and K-type thermocouples are installed at the inlet and outlet of the minichannel. The other basic elements of the experimental setup are a data acquisition station, a computer with special software, two digital cameras and an IR camera, as shown in Fig. 1.

The surface of the heating foil that was in contact with the fluid in the minichannel was enhanced. The mini cavities (Fig. 2c) produced by spark erosion over the whole surface area of the foil using an arcograph were distributed unevenly and their dimensions varied. The rims of resolidified melt

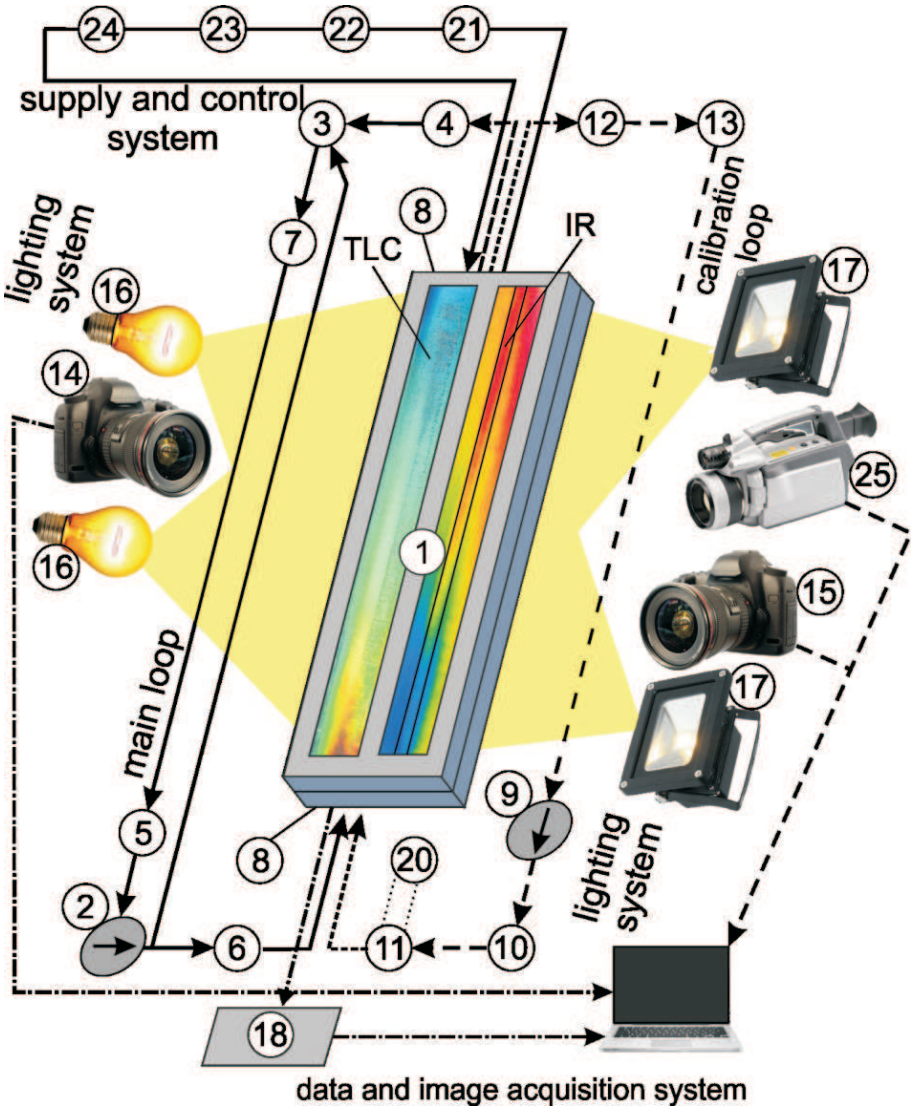

Figure 1: The schematic diagram of the main systems of the experimental setup, 1 – test section with two parallel minichannels; 2,9 – rotary pumps, 3 – compensating tank/pressure regulator, 4 – tube-type heat exchanger, 5,10,13 – filters, 6-rotameters, 7,12 – deaerators, 8 – pressure converter, 11 – heater with an electric heating element, 14 – digital camera, 15 – digital SLR camera, 16 – fluorescent lamps, 17 – halogen lamps, 18 – data acquisition station, 19 – laptop, 20 – autotransformer, 21 – inverter welder, 22 – shunt, 23 – ammeter, 24 – voltmeter, 25 – infrared camera.

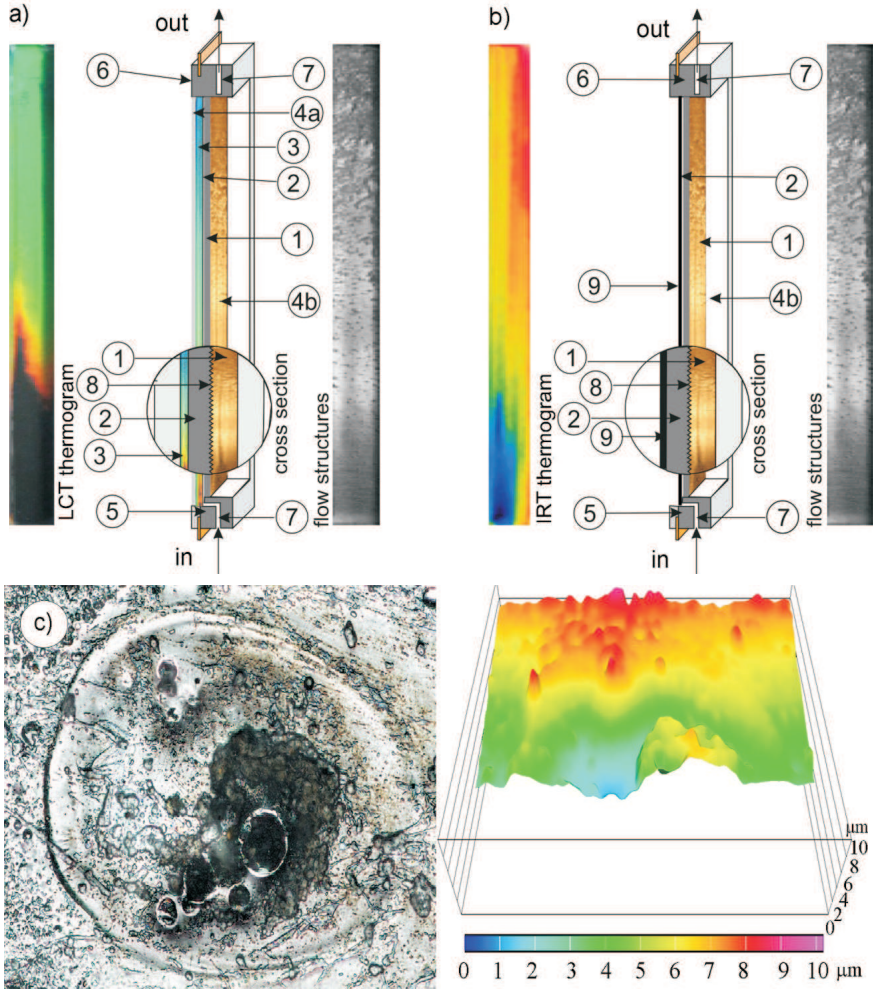

Figure 2: The schematic diagrams of the test section with: a) the LCT minichannel; b) the IRT minichannel: 1 – minichannel, 2 – heating foil, 3 – liquid crystal layer, 4a,b – glasspanels, 5 – channel body, 6 – front cover, 7 – thermocouple, 8 – enhanced surface of the foil, 9 – black paint layer; c) foil surface enhanced by spark erosion; fragment with minicavities: image and 3D topography.

from the electrode and the foil were several μm in height, with a maximum height being 5 μm. The craters were usually less than 1 μm deep.

3 Test methodology

The testing requires that a calibration procedure is performed first. Its aim is to determine the hue-temperature relationship, i.e., to correlate the colour response to the temperature of the foil surface [46,51]. The actual test with a refrigerant in the system begins with degasification. After the deaeration, the working fluid (FC-72) flows laminarly along the minichannel.

Measurements consist of photographing the minichannels simultaneously from both sides: with a digital camera(LCT minichannel) and an infrared camera(IRT minichannel) to monitor the temperature on the smooth surface and with a digital camera to record the flow structures on the enhanced surface. Once switched on, an infrared camera self-calibrates. However, it is necessary to set, for example, the object emissivity, the distance to the object, the ambient temperature, and the relative humidity. For digital cameras, it is vital first to set the distance from the object, then focus, and finally ensure stability to be able to take repetitive images, in order to monitor the changes in the process. Data collected with the infrared camera are recorded in the form of IR thermograms.

When the desired pressure and flow rate are reached, there is a gradual increase in the electric power supplied to the heating foil followed by an increase in the heat flux transferred to the fluid in the channel. This leads to the onset of nucleate boiling and the heat transfer enhancement. After the maximum current is achieved (with the value dependent on the operating temperature range of the liquid crystal display), there is a gradual decrease in the heat flux supplied to the heating foil. It takes longer for the heat flux to decline while the current is decreased than when it is increased. And this is due to higher thermal inertia of the metal elements of the experimental setup. As all the measurements were performed under stable thermal and flow conditions at a constant heat flux supplied to the heating surface, the results correspond to steady-state regimes.

4 Aim and methodology of the calculations

The aim of the calculations was to evaluate the suitability of the one dimensional model for determining the heat transfer coefficient at the foil-fluid interface. In this model, local values of the heat transfer coefficient in the area between the heating foil and the boiling fluid are calculated from the Robin boundary condition (third-kind boundary condition). Under this

condition,the rate of heat transfer by convection between the multilayer wall and the moving liquid is equal to the rate of heat transfer by conduction between the liquid and the wall. In this study, flow boiling heat transfer was analyzed using two contactless measurement techniques: liquid crystal thermography and infrared thermography. The results obtained by the above methods were represented graphically as relationships between the foil temperature and the distance from the minichannel inlet and between the heat transfer coefficient and the distance from the minichannel inlet.

Convection is a mechanism of heat transfer between a solid surface and a fluid or gas in motion. The process involves the combined effect of fluid motion and conduction. This mechanism of heat transfer is strongly dependent on the fluid properties (density, thermal conductivity, dynamic viscosity, specific heat or velocity), the type of fluid flow (laminar or turbulent), and finally the geometry or roughness of the heating element. The rate of convection heat transfer is observed to be proportional to the temperature difference and is described by Newton's law as

$$q_{w(conv)} = \alpha(T_w - T_f)\,, \tag{2}$$

where: α – is local values of the heat transfer coefficient, T_w – wall temperature, T_f – fluid temperature.

The heat is transfered from the solid surface to the fluid layer by conduction. As the fluid layer is stationary, it can be described as

$$q_{w(conv)} = q_{w(cond)} = -\alpha\frac{\partial T}{\partial n}\,, \tag{3}$$

where: ∂T – temperature derivative, ∂n – derivative of temperature in the direction normal to the isothermal surface [52,53].

5 Estimation of the heat loss

As the central part, 10 mm × 350 mm rectangle, of the heating foil where the surface temperature is measured with the infrared camera (Fig. 3b) is not insulated, the loss of heat to the surroundings is the greatest. The results of the heat loss measurements conducted for each current setting indicate that the greatest heat loss occurs at the highest heat flux, while the smallest is observed at the minimum heat flux. The average loss of heat to the surroundings for the analyzed measurement series was 1.3% of the heat flux density (taken into account in Eq. (5)). It is obvious that the loss

is relatively small because the measuring module itself is quite small.

The issue of heat loss for a minichannel was discussed in [36]. They were considered to be negligible and omitted in the calculations. Similar observations were reported for the IRT minichannel.

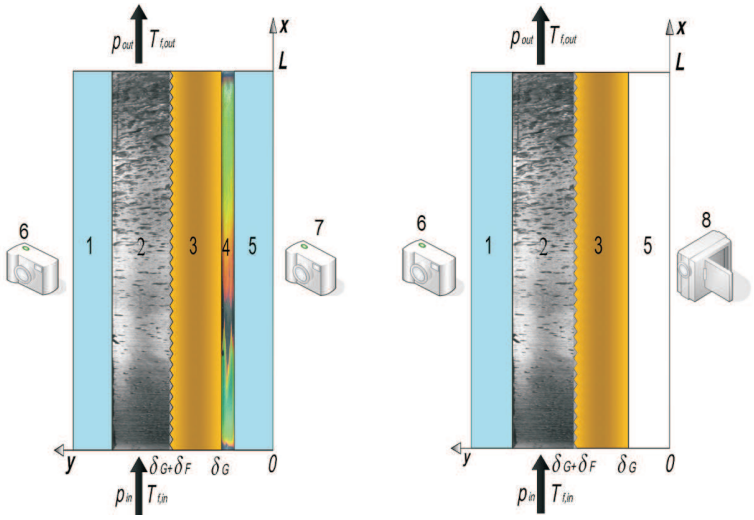

Figure 3: The schematic diagram of the main elements of the central part of the test section with the LCT minichannel (a); the IRT minichannel (b): 1, 5 – glass panels, 2 – minichannel, 3 – heating foil, 4 – liquid crystal layer, 6 – SLR digital camera, 7 – digital camera, 8 – thermal imaging camera.

6 Determination of the heat transfer coefficient

When the one-dimensional model is used, first it is necessary to calculate the heat transferred to the fluid separately for each minichannel by using the heating foil temperature determined by liquid crystal thermography and infrared thermography. This model takes into account the heat flow direction, which is perpendicular to the direction of the fluid flow in the minichannel. Thus, the heat transferred to the fluid in the LCT minichannel (see Fig. 3a) is equal to the heat generated by the heating foil in the this minichannel:

$$q_{w\,LCT}(x) = \frac{I\Delta U}{A_{F\,LCT}}\,, \tag{4}$$

where: I – current, ΔU – voltage drop, $A_{F\,LCT}$ – surface area of the heating foil in the LCT channel.

The amount of heat transferred to the fluid in the IRT minichannel (see Fig. 3b), which is equal to the difference between the heat generated by the heating foil and the heat lost to the surroundings, q_{wl}, is proportional to the surface area of the heating foil in the IRT minichannel:

$$q_{w\,IRT}(x) = \frac{I\Delta U}{A_{F\,IRT}} - q_{wl}\,, \tag{5}$$

where: $A_{F\,IRT}$ – surface area of the heating foil in the IRT channel, q_{wl} – is heat lost to the surroundings in the IRT minichannel.

Local values of the heat transfer coefficient in the area between the heating foil and the boiling liquid determined by LCT, $\alpha_{LCT}(x)$, are calculated from Newton's law

$$q_{w\,LCT}(x) = \alpha_{LCT}(x)\left[T_F^{LCT}(x,\,\delta_G+\delta_F) - T_{sat}(x)\right], \tag{6}$$

where: $T_F^{LCT}(x,\,\delta_G+\delta_F)$ – the foil temperature measured by liquid crystal thermography, $T_{sat}(x)$ – liquid saturation temperature determined on the basis of the linear distribution of pressure along the length of the minichannel from the inlet to the outlet.

It is assumed that $T_F^{LCT}(x,\,\delta_G+\delta_F) = T_F^{LCT}(x,\,\delta_G)$. The temperature gradient through the heating foil thickness was not taken into consideration due to very low values. Temperature $T_F^{LCT}(x,\,\delta_G+\delta_F)$ was derived using Fourier's law, which describes heat conduction through the foil. It is assumed that the application of simplification $T_F^{LCT}(x,\,\delta_G+\delta_F) = T_F^{LCT}(x,\,\delta_G)$ has a very slight impact on the values of the heat transfer coefficient because the foil is very thin.

Local values of the heat transfer coefficient in the area between the heating foil and the boiling fluid determined by IRT, $\alpha_{IRT}(x)$, are calculated from Newton's law:

$$q_{w\,IRT}(x) = \alpha_{IRT}(x)\left[T_F^{IRT}(x,\,\delta_G+\delta_F) - T_{sat}(x)\right], \tag{7}$$

where: $T_F^{IRT}(x,\,\delta_G+\delta_F)$ - the foil temperature measured by infrared thermography, thus by analogy to the LCT case, $T_F^{IRT}(x,\,\delta_G+\delta_F) = T_F^{IRT}(x,\,\delta_G)$.

Finally, local values of the heat transfer coefficient are calculated as follows:

- for the LCT minichannel

$$\alpha_{LCT}(x) = \frac{q_{w\,LCT}(x)}{T_F^{LCT}(x,\,\delta_G) - T_{sat}(x)}\,, \tag{8}$$

- for the IRT minichannel

$$\alpha_{IRT}(x) = \frac{q_{w\,IRT}(x)}{T_F^{IRT}(x,\,\delta_G) - T_{sat}(x)}\ . \tag{9}$$

7 Measurement errors

The accuracy of the measurements of the heating foil temperature by liquid crystal thermography was assessed by determining the error in the measurement of the heat source efficiency for the same experimental setup with a single rectangular minichannel [46,51]. The relative error was 3.53%. The mean error in the measurement of the heating foil temperature using liquid crystal thermography was approximately 0.86 K. The images taken with a FLIR SC640 infrared camera system operating in the spectral range from 7.5 μm to 13 μm were recorded in a digital system with an image frequency of 30 Hz. The accuracy of the camera was $\pm$ 2 °C or $\pm$ 2%. The camera can be used for remote real time measurement of temperature with a thermal resolution ranging from 273.21 K to 303.15 K [54].

8 Results

The experimental results are shown in the form of thermograms of the heating foil surface obtained by liquid crystal thermography (Fig. 4a) and infrared thermography (Fig. 4b) for 145 kg/(m^{2}s) mass flux, 160 kPa inlet pressure and 45 K inlet liquid subcooling. The measurement results represented as relationships between the heating foil temperature and the distance along the length of the minichannel obtained by LCT and IRT are shown in Figs. 5a and 5b, respectively. The values of the heat transfer coefficient plotted against the distance from the minichannel inlet calculated using the one-dimensional model are presented in Figs. 6a and 6b. The calculations took into account only the data obtained for saturated boiling. The results for subcooled boiling and the incipience of boiling were discussed in [38–40,46,47,55].

Figure 5 shows the distribution of temperature on the heating surface against the distance from the minichannel inlet measured with liquid crystal thermography (Fig. 5a) and infrared thermography (Fig. 5b) for the same heat flux supplied to the heating surface. The values of the temperature obtained through liquid crystal thermography were measured within the operating range, i.e., approx. from 333 K to 353 K. That is why only a selected

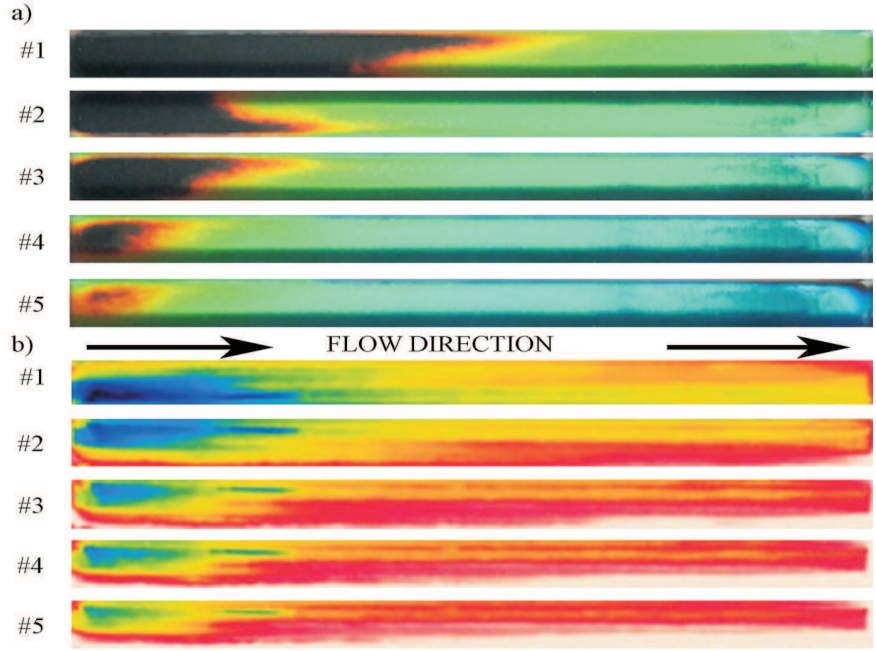

Figure 4: Thermograms of the heating foil surface obtained by liquid crystal thermography, (a) and infrared thermography (b) at the following parameters: mass flux 145 kg/(m^{2}s), inlet pressure 160 kPa, inlet liquid subcooling 45 K; 1) q_w = 10883 W/m^2, 2) q_w = 12597 W/m^2, 3) q_w = 14233 W/m^2, 4) q_w = 15669 W/m^2, 5) q_w = 16387 W/m^2.

section of the channel was studied. On the other hand, the results obtained through infrared thermography always showed the temperature of the heating surface for the whole length of the minichannel. The LCT measurement data for the parts located closest to the inlet and outlet (approx. 15% at each end) was omitted in the analysis. For these results, the measurement error was the highest and it was attributable to the calibration procedure, the aim of which is to determine the hue-temperature relationship. Details of the calibration procedure were discussed in [46,51].

The temperature trends in both graphs indicate that when the heat flux supplied to the heating surface rises there is a gradual increase in the surface temperature. The IRT results (Fig. 5b) show that locally the temperature of the foil surface at the minichannel outlet decreases; this is due to the fact that there is a direct contact of the channel walls with the cooler parts of the module. The comparative analysis of the graphical data obtained with

the two contactless measurement methods demonstrates that the values of temperature are similar. The greatest differences were reported for # 5 of the heat flux setting, at which the temperature measured by LCT was about 5 K lower than that obtained with IRT.

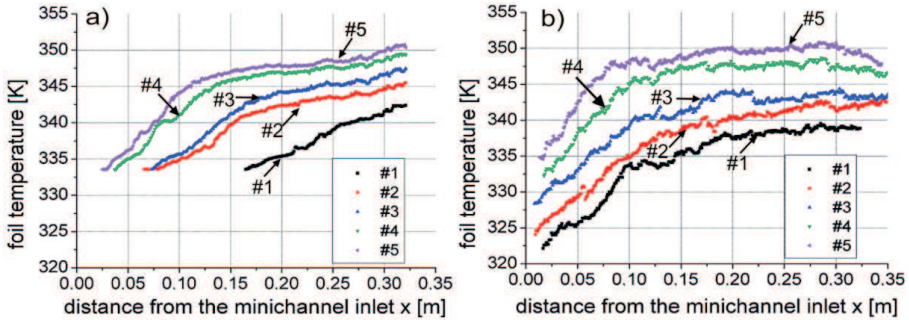

a) b)

Figure 5: Heating foil temperature vs. the distance along the length of the minichannel determined experimentally by liquid crystal thermography (a), infrared thermography (b), with parameters the same as in Fig. 4.

Figure 6 illustrates the heat transfer coefficient against the distance from the minichannel inlet obtained on the basis of the one-dimensional model using the temperature data recorded by IRT (Fig. 6a) and LCT (Fig. 6b). This paper analyzes the local values of the heat transfer coefficient only for saturated boiling. In the saturated nucleate boiling region, the heat transfer coefficient decreases considerably with an increase in the distance from the channel inlet, which is accompanied by an increase in the vapour volume fraction in the mixture. The values of the heat transfer coefficient recorded at the minichannel outlet are lower than the highest values observed closer to the minichannel inlet. As the heat flux supplied to the heating foil is reduced, the heat transfer in the minichannel returns to single phase forced convection with the values of local heat transfer coefficient being low and approximately constant. The lowest values of the coefficient were reported at the channel outlet while single-phase convection takes place (as seen in Fig. 6a).

It should be noted that the heat transfer coefficient trends for the two contactless methods are similar. In both cases, the curves slope downwards as the distance from the inlet increases. However, there was a large scatter of results when the heat transfer coefficient was determined by IRT (particularly for # 1, # 2). It was also found that local values of the coefficient

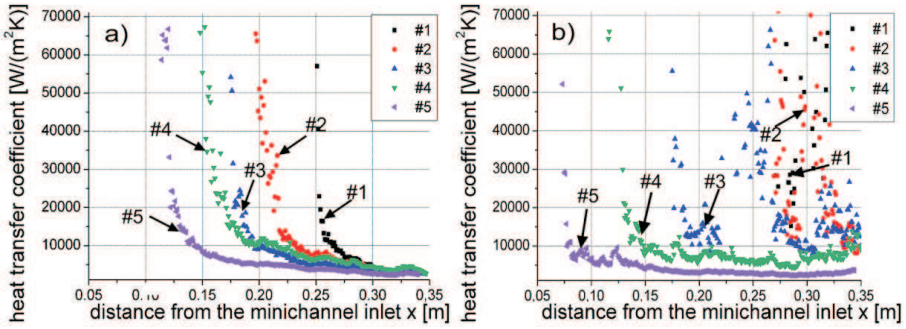

a) b)

Figure 6: Heat transfer coefficient vs. the distance along the length of the minichannel determined on the basis of the one-dimensional model from the measurement data: a) liquid crystal thermography, b) infrared thermography, with parameters the same as in Fig. 4.

recorded through IRT at the minichannel inlet were shifted to the left side (see Fig. 6) in comparison with the LCT data.

The comparative analysis indicates that the values of the heating surface temperature recorded with the two contactless measurement methods were similar. Figures 5a and 5b show the distribution of the temperature of the heating surface along the length of the minichannel from the inlet for liquid crystal thermography and infrared thermography, respectively. As can be seen, the distributions of temperature measured by LCT and IRT are similar for different heat flux settings. a marked difference in temperature between the two methods of measurement was reported for # 1 heat flux setting, when the temperature measured by LCT was lower than that obtained with IRT.

9 Statistical analysis

The differences between two sets of measurement data concerning the temperature of the heating surface obtained with LCT and IRT were analyzed using the Student's t-test. This method enabled us to assess whether the temperature variances obtained with the two techniques were equal. It was assumed that the distributions of results in each set resemble the normal distribution. The study was conducted at two settings of the heat flux for the following section lengths: 0.165–0.32 m (# 1) and 0.075–0.32 m (# 3). With the level of significance of 0.05 for a two-sided test, the probability

that the statistic will be less than or equal to the critical value is 0.91 and 0.09 for (# 1) and (# 3), respectively. The results indicate that the hypothesis that the two variances are equal for all the features tested cannot be rejected [56].

The analysis of the relationship between the heat transfer coefficient and the distance along the length of the minichannel indicates that the heat transfer coefficient decreases rapidly in the boiling region. For higher volume fractions of the vapour phase in the two-phase mixture during nucleate saturated boiling, the heat transfer coefficient decreases gradually. The values at the minichannel outlet are lower than the highest values recorded closer to the minichannel inlet. From a statistical analysis of the measurement data it was evident that the temperature variances obtained for a given series with the two methods were the same for the selected settings of the heat flux.

The values of the heat transfer coefficient obtained by IRT and LCT plotted against the distance along the length of the minichannel were calculated using the one-dimensional model. The results are graphically represented in Fig. 6. As can be seen, all the curves slope downwards. However, the results of infrared thermography, especially those for # 1 and # 2, show a large scatter. The values of the coefficient obtained by IRT are shifted to one side when compared with those determined by the LCT method.

10 Conclusions

The simultaneous use of the two techniques for contactless measurement of surface temperature, i.e., liquid crystal thermography and infrared thermography, enabled us to obtain more comprehensive data on the heat transfer coefficient. As a result, it was possible to compare the foil surface temperature with the heat transfer coefficient for saturated boiling. The paper has shown the relationships between the temperature of the heating foil measured by LCT and IRT and the distance from the inlet to the outlet of the minichannel for five values of the heat flux supplied to the foil. From the local values of the temperature obtained by LCT and IRT it is clear that the distributions of temperature over the heating surface recorded at different values of the heat flux were similar. However, infrared thermography provided more detailed data for the whole length of the minichannel. The values of the heat transfer coefficient plotted against the distance from the minichannel inlet are similar for both methods. The curves slope down-

wards as the refrigerant flows through the minichannel. Nevertheless, the IRT method is characterized by fairly scattered values.

Acknowledgment The research reported herein was supported by a grant from the National Science Centre (No. DEC-2013/09/B/ST8/02825).

Received 16 March, 2015

References

[1] Piasecka M., Maciejewska B.: *Enhanced heating surface application in a minichannel flow and the use of the FEM and Trefftz functions for the solution of inverse heat transfer problem.* Exp. Therm. Fluid Sci. **44**(2013), 23–33.

[2] Saisorn S., Kaew-On J., Wongwises S.: *An experimental investigation of flow boiling heat transfer of R-134a in horizontal and vertical minichannels.* Exp. Therm. Fluid Sci. **46**(2013), 232-244.

[3] Kandlikar S.G., Grande W.J.: *Evolution of microchannel flow passages-thermohydraulic performance and fabrication technology.* Heat Transfer Eng. **25**(2002), 3–17.

[4] Shah R.K.: *Classification of Heat Exchangers.* Hemisphere, Washington DC, 1981, 9-46.

[5] Kew P.A., Cornwell K.: *Correlations for the prediction of boiling heat transfer in small diameter channels.* Appl. Therm. Eng. **17**(1977), 705–715.

[6] Bohdal T: *Bubbly boiling of environmental-friendly refrigerating media.* Int. J. Heat Fluid Fl. **21**(2000), 4, 449–455.

[7] Bohdal T.: *Development of bubbly boiling in channel flow.* Exp. Heat Transfer **4**(2001), 199–215.

[8] Bohdal T., Kuczyński W.: *Investigation of boiling of refrigerating medium under conditions of impulse disturbances.* Exp. Heat Transfer **17**(2004), 2, 103–117.

[9] Bohdal T., Charun, H., Sikora M.: *Comparative investigations of the condensation of R134a and R404A refrigerants in pipe minichannels.* Int. J. Heat Mass Tran. **54**(2011), 1963–1974.

[10] Kuczyński W., Bohdal T., Charun H.: *Impact of periodically generated hydrodynamic disturbances on the condensation efficiency of R134a refrigerant in pipe mini-channels.* Exp. Heat Transfer **26**(2013), 1, 64–84.

[11] Kuczyński W., Charun H., Bohdal T.: *Influence of hydrodynamic instability on the heat transfer coefficient during condensation of R134a and R404A refrigerants in pipe mini-channels.* Int. J. Heat Mass Tran. **55**(2012), 4, 1083–1094.

[12] Dutkowski K: *Experimental investigations of Poiseuille number laminar flow of water and air in minichannels.* Int. J. Heat Mass Tran. **51**(2008), 5983–5990.

[13] Dutkowski K.: *Two-phase pressure drop of air-water in minichannels.* Int. J. Heat Mass Tran. **52**(2009), 5185–5192.

[14] Dutkowski K.: *Influence of the flashing phenomenon on the boiling curve of refrigerant R134a in minichannels.* Int. J. Heat Mass Tran. **53**(2010), 1036–1043.

[15] Dutkowski K.: *Single phase pressure drop in minichannels.* Transactions IFFM **121**(2008), 17–32.

[16] Mikielewicz D., Mikielewicz J., Tesmar J.: *Improved semi-empirical method for determination of heat transfer coefficient in flow boiling in conventional and small diameter tube.* Int. J. Heat Mass Tran. **50**(2007), 3949–3956.

[17] Mikielewicz D.: *A new method for determination of flow boiling heat transfer coefficient in conventional-diameter channels and minichannels.* Heat Transfer Eng. **31**(2010), 276–287.

[18] Mikielewicz D., Mikielewicz J.: *A common method for calculation of flow boiling and flow condensation heat transfer coefficients in minichannels with account of nonadiabatic effects.* Heat Transfer Eng. **32**(2011), 1173–1181.

[19] Mikielewicz D., Klugmann M., Wajs J.: *Experimental investigation of M-shape heat transfer coefficient distribution of R123 flow boiling in small-diameter tubes.* Heat Transfer Eng. **33**(2012), 584–595.

[20] Cieśliński J.T.: *Nucleate pool boiling on porous metallic coatings.* Exp. Therm. Fluid Sci. **25**(2002), 7, 557–564.

[21] Cieśliński J., Krasowski K.: *Heat transfer during pool boiling of water, methanol, and R141B on porous coated horizontal tube bundles.* J. Enhanc. Heat Tran. **20**(2013), 2, 165–177.

[22] Cieśliński J.T., Targański W.: *Investigation of R22 and R134a flow boiling in enhanced tubes.* Transactions IFFM **112**(2003), 21–36.

[23] Dawidowicz B., Cieśliński J.: *Heat transfer and pressure drop during flow boiling of pure refrigerants and refrigerant/oil mixtures in tube with porous coating.* Int. J. Heat Mass Transf. **55**(2012), 9-10, 2549–2558.

[24] Cieśliński J.T.: *Flow and pool boiling on porous coated surfaces.* Rev. Chem. Eng. **27**(2011), 179–190.

[25] Wilk J.: *Convective mass/heat transfer in the entrance region of the short circular minichannel.* Exp. Therm. Fluid Sci. **38**(2012), 107–114

[26] Wilk J.: *Experimental investigation of convective mass/heat transfer in short minichannel at low Reynolds numbers.* Exp. Therm. Fluid Sci. **33**(2009), 267–272.

[27] Ciałkowski M.J., Frąckowiak A.: *Heat Functions and their Use in Solving Problems of Thermal Conductivity and Mechanics.* Poznań University of Technology, Poznań 2002.

[28] Orzechowski T.: *Determining local values of the heat transfer coefficient on a fin.* Exp. Therm. Fluid Sci. **31**(2007), 8, 947–955.

[29] Orzechowski T., Tyburczyk A.: *Two-phase cooling efficiency on the basis of fin with mesh structure.* Exp. Therm. Fluid Sci. **87**(2011), 7, 48–51.

[30] Orzechowski T., Tyburczyk A.: *Boiling heat transfer on fins – experimental and numerical procedure.* EPJ Web of Conf. **67**(2014), 02088.

[31] Wójcik T.M: *Experimental investigations into intra-layer boiling crisis and hysteresis in metal. Fibrous.* Transactions IFFM **112**(2003), 91–102.

[32] Wójcik T.M., Poniewski M.E.: *Experimental investigation and modeling of boiling heat transfer hysteresis on porous surfaces.* J. Enhanc. Heat Tran. **5**(2008), 4, 289–301.

[33] Wójcik T.M.: *Boiling heat transfer on new capillary-porous coverings.* In: Proc. Int. Conf. on Exp. Fluid Mech. Liberec, Nov. 25-27, 2009, 426–431.

[34] Pastuszko R.: *Temperature field in the-layer fins immersed in boiling water.* Transactions **112**(2003), 103–118.

[35] Pastuszko R.: *Boiling heat transfer enhancement in subsurface horizontal and vertical tunnels.* Exp. Therm. Fluid Sci. **32**(2008), 1564–1577.

[36] Pastuszko R.: *Pool boiling on micro-fin array with wire mesh structures.* Int. J. Therm. Sci. **49**(2010), 2289–2298.

[37] Pastuszko R.: *Pool boiling for extended surfaces with narrow tunnels – Visualization and a simplified model.* Exp. Therm. Fluid Sci. **38**(2012), 149–164.

[38] Piasecka M., Hożejowska S., Poniewski M.E.: *Experimental evaluation of flow boiling incipience of subcooled fluid in a narrow channel.* Int. J. Heat Fluid Fl. **25**(2004), 159–172.

[39] Piasecka M., Poniewski M.E.: *Hysteresis phenomena at the onset of subcooled nucleate flow boiling in microchannels.* Heat Transfer Eng. **25**(2004), 3, 44–51.

[40] Piasecka M., Poniewski M.E.: *Flow boiling incipience in minichannels.* In: Proc. 3rd Int. Symp. on Two-phase Flow Modelling and Experimentation, Pisa 2004 (CD-ROM–8, mt-13).

[41] Piasecka M.: *Heat transfer mechanism, pressure drop and flow patterns during FC-72 flow boiling in horizontal and vertical minichannels with enhanced walls.* Int. J. Heat Mass Tran. **66**(2013), 72–488.

[42] Piasecka M.: *An application of enhanced heating surface with mini-recesses for flow boiling research in minichannels.* Heat Mass Tran. **49**(2013), 261–271.

[43] Piasecka M.: *Flow boiling heat transfer in a minichannel with enhanced heating surface.* Heat Transfer Eng. **35**(2014), 10, 903–912.

[44] Piasecka M.: *The use of enhanced surface in flow boiling heat transfer in a rectangular minichannels.* Exp. Heat Transfer **27**(2014), 231–255.

[45] Piasecka M.: *Correlations for flow boiling heat transfer in minichannels with various orientations.* Int. J. Heat Mass Tran. **81**(2015), 114–121.

[46] Piasecka M., Maciejewska B.: *The study of boiling heat transfer in vertically and horizontally oriented rectangular minichannels and the solution to the inverse heat transfer problem with the use of the Beck method and Trefftz functions.* Exp. Therm. Fluid Sci. **38**(2012), 19–32.

[47] Piasecka M., Maciejewska B.: *Enhanced heating surface application in a minichannel flow and use the FEM and Trefftz functions to the solution of inverse heat transfer problem.* Exp. Therm. Fluid Sci. **44**(2013), 23–33.

[48] Kaniowski R., Poniewski M.E.: *Measurements of two-phase flow patterns and local void fraction in vertical rectangular minichannel.* Arch. Thermodyn. **34**(2014), 2, 3–21.

[49] Hożejowska S., Kaniowski R., Poniewski M.E.: *Application of adjustment calculus to the Trefftz method for calculating temperature field of the boiling liquid flowing in a minichannel.* Int. J. Numer Method. H. **24** (2014), 811–824.

[50] Orzechowski T.: *Heat transfer on ribs with microstructured surface.* Kielce University of Technology, Monographs, Studies, Hearings **39**(2003) (in Polish).

[51] Piasecka M.: *Determination of the temperature field using liquid crystal thermography and analysis of two-phase flow structures in research on boiling heat transfer in a minichannel.* Metrol. Meas. Syst. **20**(2013), 2, 205–216.

[52] Yunus A., Cengel, Turner R. H.: *Fundamentals of Thermal-fluid Sciences.* McGraw – Hill Higher Education, 2001.

[53] Wiśniewski S., Wisniewski T.S.: *Heat Transfer.* WNT, Warsaw 2012 (in Polish).

[54] *User's manual ThermaCam B640, P640, SC640.* Publ. No. 155850 Rev.a 201-ENGLISH (EN), 2007.

[55] Piasecka M..: *Correlations for flow boiling heat transfer in minichannels with various orientations.* Heat Mass Transfer **50**(2014), 1053–1063.

[56] Krysicki W.: *Probability theory and mathematical statistics. Practice exercises, Part 2.* PWN, Warsaw 2000 (in Polish).